Tropical Cyclone Seeds, Transition Probabilities, and Genesis

KERRY EMANUEL[a]

[a] *Lorenz Center, Massachusetts Institute of Technology, Cambridge, Massachusetts*

(Manuscript received 1 December 2021, in final form 5 February 2022)

ABSTRACT: It has been proposed that tropical cyclogenesis rates can be expressed as the product of the frequency of "seeds" and a transition probability that depends on the large-scale environment. Here it is demonstrated that the partitioning between seed frequency and transition probability depends on the seed definition and that the existence of such a partition does not resolve the long-standing issue of whether tropical cyclone frequency is controlled more by environmental conditions or by the statistics of background weather. It is here argued that tropical cyclone climatology is mostly controlled by regional environment and that the response of global tropical cyclone activity to globally uniform radiative forcing may be more controlled by the regionality of the response than by the mean response.

KEYWORDS: Tropical cyclones; Downscaling; Climate variability

1. Introduction

The genesis of tropical cyclones remains an enduring scientific mystery. Early investigators were quick to conclude, based on observations, that tropical cyclones always develop from pre-existing disturbances of presumably independent physical origins. For example, in his review of tropical cyclones, Dunn (1951) states that "[i]n all cases of hurricane formation noted in the course of this study, deepening began, without exception, in pre-existing tropical disturbances" (p. 895). In the same volume, Riehl (1951) comments that "[s]torms never develop spontaneously in the undisturbed tropical currents but always in a preexisting disturbance" (p. 908). He also remarks, in reference to depressions of less than tropical storm intensity, that "[s]uch centers have been observed to travel in relatively steady state over distances in excess of 1000–1500 miles" (p. 907).

It is clear that most researchers believed that the pre-existing disturbances arose from processes largely independent of those that ultimately intensify tropical cyclones. For example, Dunn (1951) remarked that "[t]ropical cyclones originate in easterly waves, in the intertropical convergence zone, and occasionally in the trailing southerly portions of old polar troughs" (p. 894), although he later adds that "[t]here is as yet no generally accepted definition of exactly what synoptic situation is responsible for the formation of a tropical cyclone" (p. 895). They also recognized that to intensify into tropical cyclones, the disturbances had to take place under suitable environmental conditions. For example, Palmén (1948) showed that tropical cyclones do not develop in regions that are stable to moist convection. As Riehl and Burgner (1950) put it, "[t]he origin of tropical disturbances cannot be explained solely from the local structure of the air masses in which the vortex motion develops. A suitable combination of external forces and local conditions is necessary" (p. 247). They also emphasized that "there is a great difference between the analysis of conditions that produce the first formation of tropical lows and those that cause intensification, often rapid and violent" (p. 247). The dynamics underlying the triggering disturbances were thus thought to be very different from the physics of tropical cyclone intensification.

In the decades that followed, much research was published on the nature of the weaker disturbances that precede tropical cyclogenesis. Perhaps because most of the observations were in the North Atlantic basin, strong attention was paid to African easterly waves (AEWs), to upper-tropospheric disturbances, often of relatively small scale, and to the interaction between the two (e.g., Riehl 1945).

The paradigm that tropical cyclones develop from pre-existing disturbances of independent physical origin persists to this day. It has taken on renewed significance because it may prove central to the important problem of how tropical cyclone frequency might respond to global climate change. The question naturally arises as to whether the climate control of tropical cyclogenesis is exercised primarily through changes in the salubriousness of the large-scale environment or through changes in the nature and frequency of potential initiating disturbances (or some combination of both). One must also consider the possibility of appreciable feedbacks of tropical cyclones on climate itself, which may play a role in setting the global frequency and other metrics of tropical cyclone activity.

The evidence from routine observations, field experiments, theory, and numerical models paints an ambiguous picture of the relative importance of triggering disturbances and ambient conditions in controlling regional and global rates of tropical cyclogenesis. The first generally successful numerical simulation by Ooyama (1969) spun up initially very weak disturbances and the author showed that the model resting state was linearly unstable. Ooyama's initial condition was highly conditionally unstable, however, whereas observations show that air masses over tropical oceans are much closer to neutral stability (Betts 1982; Xu and Emanuel 1989). Axisymmetric numerical simulations initialized in a conditionally neutral atmosphere without water vapor– or cloud-dependent radiation (e.g., Rotunno and Emanuel 1987; Emanuel 1989) require finite-amplitude initial

Denotes content that is immediately available upon publication as open access.

Corresponding author: K. Emanuel, emanuel@mit.edu

DOI: 10.1175/JCLI-D-21-0922.1

perturbations to produce amplifying vortices, supporting the idea that the real tropical atmosphere requires finite-amplitude triggers to produce tropical cyclones, and suggesting that rates of genesis should be at least partially controlled by the abundance of potential initiating disturbances of independent origin. The initial intensification of disturbances is inhibited by the import into the boundary layer of low moist static energy by downdrafts driven by the evaporation of rain into the initially unsaturated air in the lower to middle troposphere. The degree of inhibition was shown by Emanuel (1989) to be proportional to the saturation deficit of the lower to middle troposphere. Only when the inner core of the incipient disturbance becomes saturated, or nearly so, will it begin to intensify through surface enthalpy fluxes (Emanuel 1989; Rappin et al. 2010).

Yet many three-dimensional numerical experiments with more realistic physics, carried out in idealized environments, are able to produce tropical cyclones spontaneously (Bretherton et al. 2005; Held and Zhao 2008; Nolan et al. 2007; Khairoutdinov and Emanuel 2013), probably aided by the cloud–radiation interactions that have been shown to drive self-aggregation of convection (Wing et al. 2016). This simulated spontaneous cyclogenesis has been shown to be delayed or inhibited entirely by wind shear (Rappin et al. 2010)

A line of evidence favoring the importance of environmental conditions in controlling tropical cyclone frequency is the success of various genesis indices (e.g., Gray 1975; DeMaria et al. 2001; Emanuel and Nolan 2004; Emanuel 2010; Tippett et al. 2011) in predicting spatial, seasonal, and interannual variability of tropical cyclones, including ENSO effects (Camargo et al. 2007). These indices typically use monthly mean quantities including potential intensity, saturation deficit, wind shear, and ambient vorticity. They do not include direct measures of mesoscale or synoptic-scale variability. Their success indicates some degree of environmental control on genesis rates but does not rule out a role for variability in triggering disturbances.

Even in places like the tropical Atlantic Ocean between the African coast and the Lesser Antilles, where the majority of tropical cyclones develop from AEWs, it does not necessarily follow that the absence of such waves would preclude or even diminish tropical cyclogenesis. Patricola et al. (2018) used a regional model to simulate the climate of the tropical Atlantic during the very active hurricane season of 2005, running a 10-member ensemble. The model domain extended from just off the African coast to the eastern North Pacific Ocean and was forced by observed sea surface temperatures and by time-evolving lateral boundary conditions from NCEP reanalyses. The 10 simulations of a control ensemble produced, on average, 19.5 tropical cyclones, and the locations and timings of the genesis events were highly correlated among the ensemble members. However, when a 2–10-day Lanczos filter was applied at the eastern boundary of the domain, filtering out the reanalysis AEWs, nearly the same number of tropical cyclones developed but the correlations among the 10 ensemble members were strongly reduced. This result suggests that the triggering disturbances can control the location and timing of genesis events, but not their existence, even in the Atlantic main development region (MDR), where AEWs are the dominant source of tropical cyclones.

More evidence for environmental control of tropical cyclone activity comes from the success of random seeding, the first step in a technique developed by the author and colleagues (Emanuel et al. 2008) for downscaling tropical cyclones from monthly mean quantities derived from global reanalyses and climate models. This first step consists in randomly seeding the global climate state in space and time, tracking the seeds using a beta-and-advection model (Marks 1992), and deterministically calculating their time-evolving intensity using a simple, coupled ocean–atmosphere model. The small fraction of seeds that develop to tropical storm strength are regarded as the tropical cyclone climatology relevant to the global reanalysis or model that has been downscaled. Because the input consists of monthly mean quantities, the seeded state does not contain synoptic-scale or higher-frequency disturbances. Nevertheless, the technique is successful in reproducing observed spatial distributions, seasonal cycles, and, in the Atlantic, interannual variability, consistent with the notion that the large-scale environment plays an important role in tropical cyclone variability.

Despite the success of genesis indices and the aforementioned random seeding technique in reproducing much of the observed space–time variability of tropical cyclones, it is not yet possible to fully test the ability of such techniques to predict the response of tropical cyclone activity to global greenhouse gas–induced climate change. Even fairly liberal estimates of the expected response of global genesis frequency to global warming are too small to be unequivocally observed to date.[1]

Would one expect genesis indices and random seeding to fail to handle global change even though they do well for most if not all other climate signals? Possibly. One important variable in controlling tropical cyclone genesis, both in some genesis indices (e.g., Emanuel 2010) and in the intensity model used in random seeding (Emanuel et al. 2004), is the saturation deficit of the lower to middle troposphere, as represented by the nondimensional parameter χ defined in Emanuel (1995). As temperature increases, the saturation deficit increases at constant relative humidity, but in stable global climates, the tropical tropospheric temperature remains approximately invariant owing to the inability to sustain isobaric temperature gradients with small values of the Coriolis parameter (Sobel et al. 2001). While fluctuations of tropospheric moisture content can and do change saturation deficit, the temperature dependence of the quantity cannot be easily tested if the temperature itself remains constant. Indeed, in ERA5 reanalyses between 1979 and 2019, fluctuations in monthly mean values of 600-hPa saturation entropy and the χ parameter are uncorrelated. Global climate change does change the free tropical tropospheric temperature, however, and therefore the saturation deficit; fluctuations in monthly mean values of 600-hPa saturation entropy and χ are indeed highly

[1] The most extreme projected change in global frequency among those summarized in Knutson et al. (2020) is around −30% for a 2-K surface warming. The roughly 0.5-K warming that occurred between 1980 and 2020 would scale this back to about 8%. Among 5000 realizations of a starting global count of 90 cyclones and a 41-yr imposed linear trend of −8%, with random Poisson noise about the 90-storm mean, there is only a 9% chance that such a trend would be detected with a p value less than 0.05.

negatively correlated in climate models in which CO_2 increases at 1% per year. The expected increase in mean saturation deficit χ with global warming would act as an inhibition to genesis. On the other hand, the expected increase in potential intensity would act in the opposite direction. [Potential intensity is an important factor in many empirical genesis indices (e.g., Bruyère et al. 2012), suggesting that genesis depends on the amount of thermodynamic energy available, among other things.] Depending on the relative sensitivity of models and genesis indices to saturation deficit and other important environmental variables, like potential intensity, one may obtain increasing or decreasing genesis frequency (or neither).

This lack of determinacy does not imply that, in global climate change, the frequency of potential triggering disturbances would suddenly become an important factor in controlling genesis rates. Yet is it not possible to entirely rule out this outcome.

An important conceptual and practical advance in our understanding of tropical cyclogenesis was made by Vecchi et al. (2019), Sugi et al. (2020), and Hsieh et al. (2020), who looked at the climatologies of tropical cyclone and tropical cyclone "seeds" separately. Here, seeds were given various quantitative definitions all of which pertain to disturbances that precede warm core cyclones of tropical storm strength. Hsieh et al. (2020) traced seeds all the way back to nonrotating cloud clusters identified in model output in terms of the aggregation and persistence of convective precipitation. In particular, they described the net genesis rate n_{tc} in terms of three factors:

$$n_{tc} = n_s P_2 = n_c P_1 P_2, \tag{1}$$

where n_c and n_s are the frequencies of cloud clusters and tropical cyclone seeds, respectively, P_1 is the probability of transition from a cluster to a seed, and P_2 is the probability of transition of a seed to a tropical cyclone. The clusters were defined as nonrotating aggregates of convective precipitation, while the seeds were defined as cyclonic disturbances of subtropical storm strength.

Vecchi et al. (2019), Hsieh et al. (2020), and Yang et al. (2021) showed that formulations like (1) can accurately predict spatial, seasonal, and intermodel differences in genesis rates if the cluster frequencies and transition probabilities in (1) are suitably defined in terms of large-scale monthly-mean quantities. Hsieh et al. (2020) expressed the cluster frequency as a function of monthly-mean pressure velocity in the middle troposphere ω; the probability P_1 of transition to a rotating seed in terms of the ratio of the Rhines scale to a scale associated with unitary Rossby number, both defined in terms of large-scale, monthly mean flow; and the probability P_2 of transition to a tropical storm in terms of the ventilation parameter of Tang and Emanuel (2010).

In section 2, I offer an interpretation of these results and relate them to the previous work on tropical cyclogenesis discussed earlier in section 1.

2. Clusters, seeds, and tropical cyclones

A first observation about the expression (1) is that, in practice (e.g., Hsieh et al. 2020), the right-hand side is determined from monthly-mean environmental quantities and, as such, could be considered a genesis index, were it not for the sequential nature of its application to traveling disturbances. [A derivation of the genesis potential index equivalent of (1), ignoring its sequential nature, is provided in appendix A.] In particular, Hsieh et al.'s parameterization of the cluster frequency and transition probabilities has no direct information (e.g., synoptic-scale variances) about potential initiating disturbances, although any of the terms may or may not act partially as a proxy for the frequencies of independent disturbances. For example, it is well known that AEWs develop initially as instabilities of the African easterly jet (Burpee 1972) but there is nothing in genesis indices or in the formulation of the terms in (1) by Hsieh et al. that could plausibly serve as a proxy for easterly wave genesis.

And yet Vecchi et al. (2019), Hsieh et al. (2020), and Yang et al. (2021) showed that formulations like (1) work extremely well in predicting the climatologies of tropical cyclones in a wide variety of circumstances. Given that the right-hand side of (1) can almost be regarded as another genesis index, does its formulation as products of transition probabilities offer advantages over existing genesis indices?

In a word, yes. The key is the sequential interpretation of (1): First, nonrotating clusters; second, rotating clusters; and third, tropical cyclones. The separate, nonoverlapping parameterizations of each of these implies that different physics are operating in different phases of a cyclone's evolution. Although, in reality, the transitions are almost certainly not quantized, expressing them as discrete steps offers a useful conceptual and practical simplification.

There is ample evidence that different physics operates at different stages of tropical cyclogenesis. For example, Gray (1975) states that "[s]ome of the cloud cluster's enthalpy gain relative to its surroundings is due to the reduced net radiation loss of the cluster produced by its extensive layered cloud structure" (p. 20), being among the first to identify cloud-radiation interactions as important in cloud cluster development. The advent of convection-permitting simulations in small domains under idealized conditions (e.g., Bretherton et al. 2004) allowed for detailed analyses of the physics underlying spontaneous development of tropical cyclones in such simulations. For example, Rappin et al. (2010), and Wing et al. (2016) showed, in confirmation of Gray's observation, that cloud–radiation interactions are indeed important in the early stages of spontaneous tropical cyclogenesis in a cloud-permitting model. Also, naturally, the existence of some background vorticity (planetary and/or relative) is crucial for the development of a cyclonic disturbance. Ultimately, surface enthalpy fluxes become essential for the development of a reasonably intense tropical cyclone. (Although the transition to "tropical cyclone" is operationally defined in terms of surface winds speed, closed isobars, and/or other structural attributes, it could be physically defined as the transition to a cyclone powered mostly by surface enthalpy fluxes.)

What formulations like (1), genesis indices, and random seeding do not deal with are classes of disturbances whose levels of activity cannot be predicted with the monthly mean quantities used in their respective formulations. AEWs are good examples of the latter—there is nothing in any of the

predictors used in any of these formulations that could plausibly have to do with easterly wave genesis. The same might be said for the Madden–Julian oscillation and equatorially trapped waves. All of these are known to modulate tropical cyclone activity, but none has been shown to regulate their long-term climatology. Thus, seeds, in frameworks like (1), should be regarded as emerging spontaneously under conditions defined as favorable by the parameterizations of cluster frequency and cluster transition to seeds. They should not be regarded as arising from independent disturbances, like AEWs, whose statistics cannot plausibly be linked to the predictors of the cluster frequency or transition probabilities. For this reason, the success of formulations like (1) is entirely consistent with the results of Patricola et al. (2018) and with random seeding, provided the latter begins with sufficiently weak seeds and has the physics for transition to rotating clusters and to tropical cyclones.

To illustrate this point, I ran the random seeding, tracking, and intensity algorithm of Emanuel et al. (2008) for the North Atlantic over the period 1979–2019, generating 100 tropical cyclones downscaled from ERA5 reanalyses (Hersbach et al. 2020). For the narrow purposes of the present paper, I focus on the seasonal cycle of Atlantic tropical cyclones, following Yang et al. (2021).

In my standard procedure, the initial seeds are randomly distributed in both space and time, but for purposes of computational efficiency I immediately filter out seeds that occur where and when the genesis potential index, defined as in Emanuel (2010), does not exceed a relatively low threshold value. This has the effect of eliminating seeds that are over land and cold water, thus saving computational time in tracking them and calculating their intensity. The seeds have initial maximum circular component of wind with a Gaussian distribution narrowly focused around 10 kt (1 kt $\approx$ 0.51 m s^{-1}). Only those seeds that develop a maximum circular wind component in excess of 25 kt and a maximum ground-relative wind speed of at least 40 kt are retained.

For the present purposes, I compare the standard control experiment with one in which I eliminate the genesis potential index filter and set the initial circular wind component of all seeds to 10 kt. I generously retain all storms that have a maximum circular wind component that exceeds 10 kt after 2 h.

Figure 1 compares the control simulation seasonal cycle of tropical cyclones with lifetime maximum ground-relative surface winds in excess of 35 kt with that based on IBTrACS data (Knapp et al. 2010) over 1979–2019, and with the simulation with weak initial seeds. The genesis potential index (GPI) from Emanuel (2010), summed over the Atlantic MDR (6°–18°N, 20°–60°W) is also shown for comparison.

The simulated seasonal cycle is not statistically distinguishable from the observed cycle, except for underestimating the historical counts in June and November. This may reflect the compromised ability of the synthetic technique to handle storms with a significant baroclinic component. The GPI greatly overestimates activity in June and July, as also noted by Yang et al. (2021), but the synthetic technique has no trouble simulating the rapid increase of activity from May to August. Note also that the weak seed simulation of the Atlantic annual cycle is statistically indistinguishable from the control.

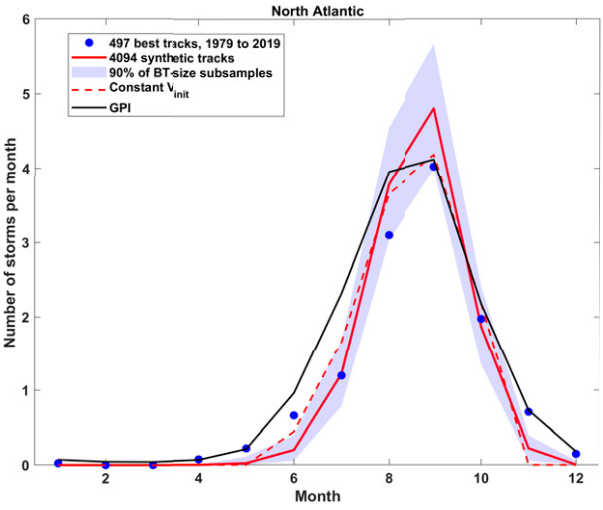

FIG. 1. Monthly average tropical cyclones over the period 1979–2019 from historical observations (blue dots), the control simulation (solid red line), the weak seed simulation (dashed red line), and a GPI summed over the North Atlantic main development region (solid black line). The blue shading shows the bounds within which lie 90% of subsamples of the control simulation, each of which has the size of the historical data.

Figure 2a shows, for the weak seed simulation, the monthly frequency of seeds whose lifetime maximum intensity (measured here by their circular wind speed) exceeds various thresholds indicated by the colored curves. Note that the seeding rate for each month is 205 per month, so that the great majority of the seeds fail to intensify from their initial circular wind maximum of 10 to even 11 kt. These seeds begin to decay immediately, having been placed in unfavorable environments.

An additional large pruning of the seeds occurs before they reach an intensity of 12 kt. With each additional increment to the lifetime maximum circular wind speed threshold, more pruning occurs until there is rough convergence at about 25 kt. (Note that, in contrast to Fig. 1, the thresholds here pertain to the circular component of wind speed. Given typical background wind speed values in the tropical North Atlantic, 25 kt of circular wind speed corresponds roughly to 35 kt of ground-relative wind speed.)

Figure 2b shows the transition probabilities associated with the frequencies in (Fig. 2s); these are defined simply as the ratio of the higher threshold frequencies to those associated with the lower threshold. As the threshold wind speed increases, the transition probabilities increase but then stabilize (and are nonmonotonic) in the 17–26-kt range. Note that the frequency of storms whose lifetime maximum wind speed exceeds the conventional tropical storm intensity of 35 kt can be expressed as the product of a seeding rate and a transition probability, with the seeding rate given by any of the curves in Fig. 2, depending on the desired definition of "seed." Clearly, the values of the seeding rate and the transition probabilities will depend on which two curves are chosen to define seeds. The gradual sharpening of the annual distribution with increasing threshold lifetime maximum intensity is consistent

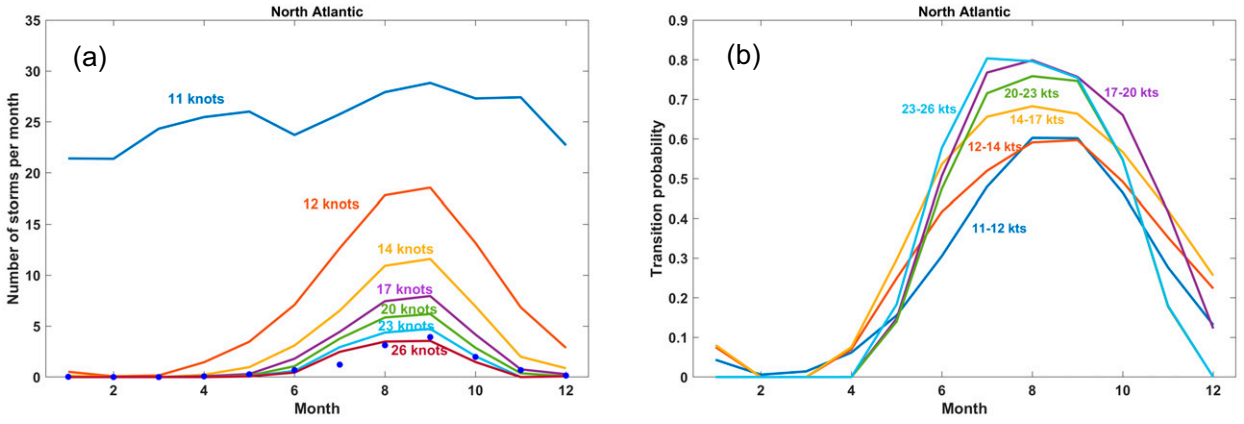

FIG. 2. (a) The annual average monthly frequency of simulated storms whose lifetime maximum circular wind speed exceeds the values labeled on the curves, from the weak seed simulation. The blue dots refer to historical observations, as in Fig. 1. The average seeding rate for each month is 205. (b) Transition probabilities associated with the frequencies shown in (a). The curves in (b) have been smoothed with a simple 1-2-1 filter.

with the results of Yang et al. (2021; see their Fig. 2), who showed that the annual distribution of seeds is somewhat flatter than that of mature cyclones.

The intensification and decay rates of the simulated tropical cyclones depend on the local potential intensity, wind shear, and midlevel saturation deficit. The relative importance of these factors undoubtedly varies with the intensity and structure of the model vortices, so the combination of these factors responsible for, say, the initial pruning to yield vortices that go on to intensify to at least 11 kt may differ from the combination that leads to further pruning of the vortices at higher intensities. While not quantized as in the formulation of (1), this evolution can be important in shaping the seasonal cycle of storms of tropical storm strength and greater. For the same reason, it is perfectly possible for some change in the climate to reduce the rate of transition of the seeds to tropical cyclones and at the same time increase the rate of transition from tropical cyclones to major hurricanes, as happens in some climate model simulations of the response to global warming (Sugi et al. 2020).

Note that in the formulation (1) developed by Hsieh et al. (2020), midlevel ω is used to parameterize nonrotating cluster frequency. But in the synthetic tropical cyclone simulator used here, ω is not an input variable. On the other hand, the seeded vortices begin with nearly saturated cores and so have, in effect, skipped the cluster development stage. The success of the technique may imply that clusters are far more plentiful than even weak tropical cyclones, so that cluster probability is only a weak determinant of cyclogenesis. Moreover, if the weak temperature gradient (WTG) approximation of Sobel et al. (2001) is used in conjunction with boundary layer quasi-equilibrium, the monthly mean midtropospheric vertical velocity is given by (Emanuel 2019)

$$w = \frac{1}{1-\epsilon_p}\left(\frac{\epsilon_p F_h}{h_b - h_m} - \frac{\dot{Q}}{S}\right), \tag{2}$$

where F_h is the surface enthalpy flux, $\dot{Q}$ is the tropospheric radiative cooling rate, h_b and h_m are the moist static energies of the boundary layer and lower middle troposphere, respectively, S is the lower tropospheric dry static stability, and ϵ_p is the convective precipitation efficiency. The denominator of the first term in parentheses in (2) can be interpreted as the saturation deficit of the lower middle troposphere because in a convectively neutral atmosphere, $h_b \simeq h^*$, where h^* is the saturation moist static energy of the troposphere (constant with height if the temperature lapse rate is moist adiabatic). Although my tropical cyclone simulator does not have background surface enthalpy flux as a predictor, it does use potential intensity, which has one factor (the air–sea thermodynamic disequilibrium) in common with surface enthalpy flux. Thus, although vertical velocity does not enter my downscaling, the latter does depend on environmental variables that, in the deep tropics, are related to vertical velocity as determined using the WTG approximation.

It should be clear from Fig. 2 that the success of random seeding depends on the initial amplitudes being small enough. To prove the point, I repeated the experiment without the GPI filter and with constant initial amplitude, but increased that amplitude from 10 to 20 kt. In this case (not shown), the seasonal cycle of tropical cyclones was very poorly simulated and other aspects of the tropical cyclone climatology were similarly poor. (The deterioration in performance is roughly linear between the 10- and 20-kt thresholds.) Therefore, for the selection mechanism to operate effectively, the initial seed amplitude must be sufficiently small.

Neither the random seeding technique nor any GPI can ever be free of a single scalar calibration constant and therefore cannot be used to explore why there are roughly 90 tropical cyclones over the globe in an average year in the current climate. This is also true of the formulation (1), as noted by Hsieh et al. (2020). Yet all of these techniques are successful in explaining all well-quantified observed climate variability, such as the seasonal cycle, the geographic distribution of tropical cyclones, interannual variability, at least in the Atlantic, and the response to ENSO in various basins. In particular, random seeding is successful in accounting for all observed, well-quantified variability provided

the initial seeds are reasonably weak.[2] If, on the other hand, seeds have an initial circular winds speed of 20 kt (not shown), this is not the case, demonstrating that the attribution of climate-related changes in tropical cyclone activity to changing frequencies of seeds and changing transition probabilities depends very much on one's definition of seed. For example, Sugi et al. (2020), in their analysis of tropical cyclogenesis in global models, define seeds as warm core vortices whose surface winds are between 20 and 35 kt and find that the changes in the frequency of seeds defined in this way are important predictors of changes in tropical cyclone frequency. This would certainly also be true of synthetic tropical cyclones generated from random seeding, if the same definition of seed were used. But this in no way disproves the utility of random seeding at much smaller amplitudes.

3. Global tropical cyclone activity

The inability of random seeding or GPIs to predict global mean, annual mean tropical cyclone activity to within a multiplicative constant brings us back to the question of what controls global tropical cyclone activity in nature. I begin by considering two cases: spatially and temporally homogeneous environments, like constant sea surface temperature aquaplanets or regional domains, and environments that are highly inhomogeneous in space and/or time, as with Earth's climate.

In the case of constant sea surface temperature numerical experiments (sometimes referred to as "TC World" experiments), there is clear evidence that the equilibrium number of tropical cyclones is space-limited (i.e., limited by the number of cyclones that will fit in the domain). For example, in doubly periodic, cloud-permitting simulations with constant sea surface temperature and Coriolis parameter, the average distance between cyclone centers in statistical equilibrium scales as a deformation radius in moist adiabatic atmospheres, which varies as $(L_v q_b)^{1/2}/f$, where L_v is the latent heat of vaporization, q_b is the subcloud layer specific humidity, and f is the Coriolis parameter (Khairoutdinov and Emanuel 2013). As shown in appendix B, this scale is consistent with a scale derived by matching inner and outer wind profiles, as in Chavas and Emanuel (2014). Also, Reed and Chavas (2015) showed that the distance between TC-World cyclones exhibits large variance, as in nature (Dean et al. 2009; Chavas and Emanuel 2014). When the Coriolis parameter is allowed to vary, as in constant sea surface temperature aquaplanet experiments (e.g., Merlis et al. 2016), the equatorial Rhines scale also plays a role in tropical cyclone separation (Chavas and Reed 2019). In either case, the detailed time evolution from a quiescent initial condition to a state of statistical equilibrium must depend sensitively on the nature of the initial noise; indeed in constant f cloud-permitting simulations in a doubly periodic domain, Cronin and Chavas (2019) found that the weak noise of the initial condition amplifies into a fairly large number of small vortices before settling down into a smaller, stable number of larger cyclones in the statistical equilibrium state (see the videos in their supplementary material).

In nature, spatial and/or temporal variations in environmental conditions strongly limit the number of tropical cyclones, which are then controlled by such variations and perhaps by the availability of weather noise to initiate the disturbances. In this case, the simplest hypothesis, advanced by Hoogewind et al. (2020), is that the global frequency of tropical cyclones is still determined by the maximum packing density in space *and* time but is limited geographically and seasonally by the availability of conducive environments, as estimated by the ventilation index defined by Tang and Emanuel (2012) and applied to reanalysis data. They found that this hypothesis still overestimates the observed global tropical cyclone frequency by an order of magnitude.

Using an aquaplanet channel version of a regional weather forecast model coupled to a very simple energy balance ocean model, Vu et al. (2021) performed simulations with a full seasonal cycle of insolation. In these simulations, the annual mean frequency of tropical cyclones depends on climate parameters, such as the specified ocean mixed layer depth, which determines the amplitude of the seasonal cycle of sea surface temperature. For example, with large ocean mixed layer depth, the intertropical convergence zone does not migrate as far poleward as with shallower mixed layers, resulting in fewer cyclones, as found previously by Merlis et al. (2013); this difference is consistent with GPIs. On the other hand, global tropical cyclone activity was hardly affected by the imposition of equatorial Kelvin waves whose relative vorticity peaks at around 14° latitude, leading the authors to suggest that "the maximum potential genesis of the tropical atmosphere must be governed by some internal dynamical or energetic constraints rather than specific triggering mechanisms" (p. 8).

To explore the nature of such constraints, Vu et al. (2021) began by noting the presence of strong subseasonal variability in domain-summed genesis rates, peaking at a period of around two weeks. They then showed that the GPI they used was systematically larger at the beginning of episodes of high genesis rates than at the end of such episodes, and further showed that the reduction of GPI was largely owing to diminishing low-level vorticity and drying of the atmosphere. This latter feature was suggested by Khairoutdinov and Emanuel (2010) to provide a mechanism for the self-regulation of tropical climate by self-aggregation of convection: Increased aggregation would dry the atmosphere, owing to its relatively high precipitation efficiency (Bretherton et al. 2005); this in turn would cool the system by increased outgoing longwave radiation in the dry atmosphere, leading to a reduction of aggregation. Such a mechanism was shown by Mauritsen and Stevens (2015) to operate in a nonrotating, doubly periodic, cloud-permitting model with a slab ocean. The Vu et al. (2021) results suggest that this mechanism may also operate in more realistic settings where the aggregation takes the form of tropical cyclones, regulating the number of tropical cyclones over time. While this mechanism may regulate the global number of tropical cyclones in a given climate, it apparently does not altogether prevent this number from

[2] The results are not sensitive to variations in seed strength below roughly 10 kt, but as they become weaker the computational time increases because the selection process takes longer.

responding to climate change (e.g., changes in ocean mixed layer depth in their model).

4. Summary

Genesis potential indices and random seeding techniques are successful in accounting for all well-observed variations in tropical cyclone activity, down to subseasonal time scales. The advent of techniques that describe genesis probabilities as products of seed frequency and transition probabilities improves on GPIs by explicitly recognizing that different physics are in play at different stages of genesis. Here I showed that the success of such techniques should not necessarily be interpreted as an indication that the characteristics of weather noise (seeds) are important determinants of tropical cyclone activity. Indeed, provided that seeds are defined to be of low enough amplitude, the resulting randomly seeded tropical cyclone climatologies appear to be determined entirely by environmental conditions. This is consistent with recent numerical experiments (Patricola et al. 2018; Vu et al. 2021) that demonstrate insensitivity of tropical cyclone climatology to the characteristics of dynamically independent synoptic-scale disturbances, although such disturbances often determine the timing and location of individual genesis events. As of this writing, there is no definitive evidence that low-amplitude weather noise controls tropical cyclone climatology.

Genesis rates predicted by all of the aforementioned techniques depend on single multiplicative calibration constants that, in practice, are determined so as to yield observed global rates. This renders suspect their ability to predict changes in tropical cyclone activity brought about by global forcing. The only definitive results, bolstered by both theory and numerical simulation, pertain to domains with horizontally uniform boundary conditions, such as doubly periodic boxes and aquaplanets with constant sea surface temperature. In these cases, the space–time density of tropical cyclones is a packing problem and their intensity is determined by the global energy and entropy budgets. However, even seemingly small symmetry breaking of the boundary conditions can change these results. For example, in aquaplanet simulations, just adding a cross-equatorial oceanic heat flux changes the response of tropical cyclone frequency to increased greenhouse gas increases from negative to positive (Merlis et al. 2013).

These results suggest that the response of real-world genesis rates to globally uniform radiative forcing will be dictated more by the regionality of the climate response than to the globally uniform component of that response. For example, changes in the ocean's meridional overturning circulation may prove a far stronger influence on tropical cyclone activity (particularly in the Atlantic region) than the globally averaged climate response to globally uniform radiative forcing by, for example, increasing long-lived greenhouse gases.

The finding by Vu et al. (2021) supporting earlier speculations that tropical cyclones may have an appreciable negative feedback on GPI suggests that tropical cyclone climatology may be more stable in coupled models that properly resolve tropical cyclones than in low-resolution models or AGCMs. Thus, improved resolution of tropical cyclones in climate models may lead to better and more robust simulations of the climate system itself.

Acknowledgments. This work was supported by the National Science Foundation under Grant NSF AGS-1906768.

Data availability statement. The synthetic tropical cyclone data used in this study are available, for research purposes only, upon request to the author.

APPENDIX A

Genesis Potential Index Equivalent of Hsieh et al. (2020) Transition Probability Formulation

As stated in the main text, the formulation (1) can be expressed as a genesis potential index if its sequential nature is ignored. This is equivalent to ignoring the spatial and temporal variation of the monthly mean environmental quantities used to predict the cluster frequency and the transition probabilities, over the distance and time between cluster formation and transition to tropical cyclone. I also compare the resulting GPI, here referred to as GPI_H, with that of Emanuel (2010), denoted GPI_E.

Referring to Hsieh et al. (2020), I use the parameterization cluster frequency and the two transition probabilities given by their expressions (2)–(4), making the approximation $P_1 \simeq c_1 Z$ that they also make, where c_1 is a constant. I also use their approximation for Z as given by their expression (14): $Z = f/(\beta)^{1/2}$, where f is the Coriolis parameter and β is its meridional gradient. Last, in their parameterization of cluster frequency, I substitute large-scale vertical velocity w for large-scale pressure velocity ω.

With these approximations, the Hsieh et al. GPI can be written (to within a multiplicative constant) as

$$\mathrm{GPI}_H \approx \frac{\overline{w} f}{\sqrt{\beta}\left[1 + \left(\frac{\Lambda}{\Lambda_0}\right)^n\right]}, \tag{A1}$$

where Λ is the Tang and Emanuel (2010) ventilation index and Λ_0 and n are constants. The ventilation index is given by

$$\Lambda = \frac{V_{\mathrm{shear}} \chi}{V_p}. \tag{A2}$$

The term V_{shear} is the magnitude of the 250–850-hPa monthly mean wind shear, V_p is the monthly mean potential intensity, and χ is the nondimensional midlevel saturation deficit (see, e.g., Emanuel 2010). This can be compared with GPI_E:

$$\mathrm{GPI}_E \approx \frac{|\eta|^3 \chi^{-4/3} \max\left[\left(V_p - 35\ \mathrm{m\ s^{-1}}\right), 0\right]^3}{\left(V_{\mathrm{shear}} + 25\ \mathrm{m\ s^{-1}}\right)^4}, \tag{A3}$$

where η is the absolute vorticity. [In many applications of (A3), η is capped at some value.]

Comparing (A1) with (A3) shows that both genesis indices depend directly on some power of the Coriolis parameter (or

the absolute vorticity), directly on potential intensity, and inversely on saturation deficit and shear. However, GPI_H also depends on large-scale ascent and inversely on β. The latter may not be too influential because β does not vary greatly over tropical latitudes. Moreover, Camargo et al. (2014) found that GPI indices are not improved by including large-scale vertical velocity. Here I point out that in WTG conditions, the large-scale ascent rate is itself a function of surface fluxes and saturation deficit, as given by (2) in the main body of this paper. If I use (2) for the vertical velocity in (A1), ignoring radiative cooling and assuming that the precipitation efficiency is constant, and take $n \simeq 1$ (it is actually closer to 1.1), I obtain

$$\mathrm{GPI}_H \approx \frac{\frac{V_s}{\beta} f \chi^{-2} V_p}{\left(\frac{V_p}{\chi} + \frac{V_{\mathrm{shear}}}{\Lambda_0}\right)}, \tag{A4}$$

where I have used the aerodynamic flux formulation of the surface enthalpy flux F_h in (2):

$$F_h = C_k V_s (h_0^* - h_b), \tag{A5}$$

where C_k is an enthalpy exchange coefficient, assumed to be constant here, V_s is the near-surface wind speed, h_0^* is the saturation moist static energy of the sea surface, and h_b is the moist static energy of the boundary layer. Hsieh et al. (2020) take $\Lambda_0 = 0.014$.

Comparing (A3) and (A4) shows that, when WTG is assumed, the two GPIs depend on the same four parameters except that GPI_H also depends on V_s/β.

APPENDIX B

Spacing of Cyclones in *f*-plane TC-World Simulations

From the assumption that net radiative export of entropy is balanced by irreversible generation of entropy by frictional dissipation in the boundary layers of tropical cyclones in TC-World simulations, Khairoutdinov and Emanuel (2013) derived that the spacing D between cyclone centers in equilibrium scales as

$$D \simeq \frac{\sqrt{\epsilon L_v q_b}}{f}, \tag{B1}$$

where ϵ is the thermodynamic efficiency (surface temperature minus tropopause temperature divided by the former), L_v is the latent heat of vaporization, q_b is the boundary layer specific humidity, and f is the Coriolis parameter.

On the other hand, the physics of the outer regions of tropical cyclones (where there is little precipitation) shows that the radial profile of outer wind depends also on the radiative subsidence velocity and the surface drag coefficient (Emanuel 2004; Chavas and Emanuel 2014). Specifically, the one-dimensional Riccati equation for the radial variation of the azimuthal wind has a single, nondimensional parameter χ after the azimuthal wind has been normalized by the potential intensity V_p and the radius has been normalized by V_p/f. Here χ is defined as

$$\chi = \frac{2 C_D V_p}{w_{\mathrm{rad}}}, \tag{B2}$$

where C_D is the surface drag coefficient and w_{rad} is the downward vertical velocity just above the top of the friction layer.

When the outer wind profile that solves the Riccati equation is matched to an inner wind profile determined by inner-core physics (Chavas and Emanuel 2014), one obtains the complete radial profile of azimuthal wind.

There is some evidence that in TC-World equilibrium states the inner-core radial lengths vary as V_p/f. With this in mind, and considering that I also used V_p/f to scale the outer wind radii, it necessarily follows that the outer radius r_o at which the azimuthal wind vanishes varies as

$$r_o \sim \frac{V_p}{f} F(\chi), \tag{B3}$$

where F is some function of χ that must be found by solving the Riccati equation. I solved that equation for 12 different values of χ, for a peak wind speed equal to potential intensity, and fixed nondimensional radius of maximum winds, and found that, to an excellent approximation, $F \cong \chi^{1/2}$, for large enough values of χ. Using this and the definition of χ given by (B2), (B3) becomes

$$r_o \sim \frac{V_p}{f} \sqrt{\frac{2 C_D V_p}{w_{\mathrm{rad}}}}. \tag{B4}$$

I can find w_{rad} by insisting on thermodynamic energy balance in the clear, subsiding air in the outer region:

$$w_{\mathrm{rad}} \frac{ds}{dz} = \frac{dF_{\mathrm{rad}}}{dz}, \tag{B5}$$

where s is the dry static energy and F_{rad} is the net radiative flux. (Recall that I have defined w_{rad} to be positive downward.) Integrating (B5) from the top of the friction layer to the tropopause and ignoring vertical variations of w_{rad}, I get

$$w_{\mathrm{rad}}(s_{\mathrm{trop}} - s_b) \simeq F_{\mathrm{trop}} - F_b, \tag{B6}$$

where the subscripts trop and b stand for values at the tropopause and top of the friction layer, respectively.

Now if I assume that the temperature lapse rate is moist adiabatic and I take the specific humidity to vanish at the tropopause, then

$$s_{\mathrm{trop}} - s_b = L_v q_b. \tag{B7}$$

On the other hand, the right side of (B6) is proportional to the net entropy export of the troposphere, which I am assuming is balanced by frictional dissipation. Following

Khairoutdinov and Emanuel (2013) [see their expression (A9)], this gives

$$C_D V_p^3 \simeq \epsilon(F_{\text{trop}} - F_b). \tag{B8}$$

Now if I substitute (B7) and (B8) into (B6) and then substitute the resulting expression for w_{rad} into (B5), the latter becomes

$$r_o \sim \frac{\sqrt{\epsilon L_v q_b}}{f} = D. \tag{B9}$$

This shows that the separation distance between cyclone centers in TC-World simulations, estimated by Khairoutdinov and Emanuel (2013) using energy and entropy balance is consistent with the separation distance deduced by matching inner and outer radial scales from dynamical arguments, as in Chavas and Emanuel (2014).

REFERENCES

Betts, A. K., 1982: Saturation point analysis of moist convective overturning. *J. Atmos. Sci.*, **39**, 1484–1505, https://doi.org/10.1175/1520-0469(1982)039<1484:SPAOMC>2.0.CO;2.

Bretherton, C. S., M. E. Peters, and L. E. Back, 2004: Relationships between water vapor path and precipitation over the tropical oceans. *J. Climate*, **17**, 1517–1528, https://doi.org/10.1175/1520-0442(2004)017<1517:RBWVPA>2.0.CO;2.

——, P. N. Blossey, and M. F. Khairoutdinov, 2005: An energy-balance analysis of deep convective self-aggregation above uniform SST. *J. Atmos. Sci.*, **62**, 4273–4292, https://doi.org/10.1175/JAS3614.1.

Bruyère, C. L., G. J. Holland, and E. Towler, 2012: Investigating the use of a genesis potential index for tropical cyclones in the North Atlantic basin. *J. Climate*, **25**, 8611–8626, https://doi.org/10.1175/JCLI-D-11-00619.1.

Burpee, R. W., 1972: The origin and structure of easterly waves in the lower troposphere of North Africa. *J. Atmos. Sci.*, **29**, 77–90, https://doi.org/10.1175/1520-0469(1972)029<0077:TOASOE>2.0.CO;2.

Camargo, S. J., K. A. Emanuel, and A. H. Sobel, 2007: Use of a genesis potential index to diagnose ENSO effects on tropical cyclone genesis. *J. Climate*, **20**, 4819–4834, https://doi.org/10.1175/JCLI4282.1.

——, M. K. Tippett, A. H. Sobel, G. A. Vecchi, and M. Zhao, 2014: Testing the performance of tropical cyclone genesis indices in future climates using the HiRAM model. *J. Climate*, **27**, 9171–9196, https://doi.org/10.1175/JCLI-D-13-00505.1.

Chavas, D. R., and K. A. Emanuel, 2014: Equilibrium tropical cyclone size in an idealized state of axisymmetric radiative–convective equilibrium. *J. Atmos. Sci.*, **71**, 1663–1680, https://doi.org/10.1175/JAS-D-13-0155.1.

——, and K. A. Reed, 2019: Dynamical aquaplanet experiments with uniform thermal forcing: System dynamics and implications for tropical cyclone genesis and size. *J. Atmos. Sci.*, **76**, 2257–2274, https://doi.org/10.1175/JAS-D-19-0001.1.

Cronin, T. W., and D. R. Chavas, 2019: Dry and semidry tropical cyclones. *J. Atmos. Sci.*, **76**, 2193–2212, https://doi.org/10.1175/JAS-D-18-0357.1.

Dean, L., K. Emanuel, and D. R. Chavas, 2009: On the size distribution of Atlantic tropical cyclones. *Geophys. Res. Lett.*, **36**, L14803, https://doi.org/10.1029/2009GL039051.

DeMaria, M., J. A. Knaff, and B. H. Connell, 2001: A tropical cyclone genesis parameter for the tropical Atlantic. *Wea. Forecasting*, **16**, 219–233, https://doi.org/10.1175/1520-0434(2001)016<0219:ATCGPF>2.0.CO;2.

Dunn, G. E., 1951: Tropical cyclones. *Compendium of Meteorology*, T. F. Malone, Ed., Amer. Meteor. Soc., 887–901.

Emanuel, K. A., 1989: The finite-amplitude nature of tropical cyclogenesis. *J. Atmos. Sci.*, **46**, 3431–3456, https://doi.org/10.1175/1520-0469(1989)046<3431:TFANOT>2.0.CO;2.

——, 1995: The behavior of a simple hurricane model using a convective scheme based on subcloud-layer entropy equilibrium. *J. Atmos. Sci.*, **52**, 3960–3968, https://doi.org/10.1175/1520-0469(1995)052<3960:TBOASH>2.0.CO;2.

——, 2004: Tropical cyclone energetics and structure. *Atmospheric Turbulence and Mesoscale Meteorology*, E. Federovich, R. Rotunno, and B. Stevens, Eds., Cambridge University Press, 240 pp.

——, 2010: Tropical cyclone activity downscaled from NOAA-CIRES reanalysis, 1908–1958. *J. Adv. Model. Earth Syst.*, **2**, 1–12, https://doi.org/10.3894/JAMES.2010.2.1.

——, 2019: Inferences from simple models of slow, convectively coupled processes. *J. Atmos. Sci.*, **76**, 195–208, https://doi.org/10.1175/JAS-D-18-0090.1.

——, and D. S. Nolan, 2004: Tropical cyclone activity and the global climate system. *26th Conf. on Hurricanes and Tropical Meteorology*, Miami, FL, Amer. Meteor. Soc., 240–241.

——, C. DesAutels, C. Holloway, and R. Korty, 2004: Environmental control of tropical cyclone intensity. *J. Atmos. Sci.*, **61**, 843–858, https://doi.org/10.1175/1520-0469(2004)061<0843:ECOTCI>2.0.CO;2.

——, R. Sundararajan, and J. Williams, 2008: Hurricanes and global warming: Results from downscaling IPCC AR4 simulations. *Bull. Amer. Meteor. Soc.*, **89**, 347–368, https://doi.org/10.1175/BAMS-89-3-347.

Gray, W. M., 1975: Tropical cyclone genesis. Colorado State University Atmospheric Science Paper 234, 121 pp.

Held, I., and M. Zhao, 2008: Horizontally homogeneous rotating radiative-convective equilibria at GCM resolution. *J. Atmos. Sci.*, **65**, 2003–2013, https://doi.org/10.1175/2007JAS2604.1.

Hersbach, H., and Coauthors, 2020: The ERA5 global reanalysis. *Quart. J. Roy. Meteor. Soc.*, **146**, 1999–2049, https://doi.org/10.1002/qj.3803.

Hoogewind, K. A., D. R. Chavas, B. A. Schenkel, and M. E. O'Neill, 2020: Exploring controls on tropical cyclone count through the geography of environmental favorability. *J. Climate*, **33**, 1725–1745, https://doi.org/10.1175/JCLI-D-18-0862.1.

Hsieh, T.-L., G. A. Vecchi, W. Yang, I. M. Held, and S. T. Garner, 2020: Large-scale control on the frequency of tropical cyclones and seeds: A consistent relationship across a hierarchy of global atmospheric models. *Climate Dyn.*, **55**, 3177–3196, https://doi.org/10.1007/s00382-020-05446-5.

Khairoutdinov, M. F., and K. Emanuel, 2010: Aggregated convection and the regulation of tropical climate. *29th Conf. on Hurricanes and Tropical Meteorology*, Tucson, AZ, Amer. Meteor. Soc., P2.69, https://ams.confex.com/ams/pdfpapers/168418.pdf.

——, and ——, 2013: Rotating radiative-convective equilibrium simulated by a cloud-resolving model. *J. Adv. Model. Earth Syst.*, **5**, 816–825, https://doi.org/10.1002/2013MS000253.

Knapp, K. R., M. C. Kruk, D. H. Levinson, H. J. Diamond, and C. J. Neumann, 2010: The International Best Track Archive for Climate Stewardship (IBTrACS): Unifying tropical

cyclone best track data. *Bull. Amer. Meteor. Soc.*, **91**, 363–376, https://doi.org/10.1175/2009BAMS2755.1.

Knutson, T., and Coauthors, 2020: Tropical cyclones and climate change assessment. Part II: Projected response to anthropogenic warming. *Bull. Amer. Meteor. Soc.*, **101**, E303–E322, https://doi.org/10.1175/BAMS-D-18-0194.1.

Marks, D. G., 1992: *The Beta and Advection Model for Hurricane Track Forecasting.* Natl. Meteor. Center, 89 pp.

Mauritsen, T., and B. Stevens, 2015: Missing iris effect as a possible cause of muted hydrological change and high climate sensitivity in models. *Nat. Geosci.*, **8**, 346–351, https://doi.org/10.1038/ngeo2414.

Merlis, T. M., M. Zhao, and I. M. Held, 2013: The sensitivity of hurricane frequency to ITCZ changes and radiatively forced warming in aquaplanet simulations. *Geophys. Res. Lett.*, **40**, 4109–4114, https://doi.org/10.1002/grl.50680.

——, W. Zhou, I. M. Held, and M. Zhao, 2016: Surface temperature dependence of tropical cyclone-permitting simulations in a spherical model with uniform thermal forcing. *Geophys. Res. Lett.*, **43**, 2859–2865, https://doi.org/10.1002/2016GL067730.

Nolan, D. S., E. D. Rappin, and K. A. Emanuel, 2007: Tropical cyclogenesis sensitivity to environmental parameters in radiative–convective equilibrium. *Quart. J. Roy. Meteor. Soc.*, **133**, 2085–2107, https://doi.org/10.1002/qj.170.

Ooyama, K., 1969: Numerical simulation of the life-cycle of tropical cyclones. *J. Atmos. Sci.*, **26**, 3–40, https://doi.org/10.1175/1520-0469(1969)026<0003:NSOTLC>2.0.CO;2.

Palmén, E., 1948: On the formation and structure of tropical hurricanes. *Geophysica*, **3**, 26–39.

Patricola, C. M., R. Saravanan, and P. Chang, 2018: The response of Atlantic tropical cyclones to suppression of African easterly waves. *Geophys. Res. Lett.*, **45**, 471–479, https://doi.org/10.1002/2017GL076081.

Rappin, E. D., D. S. Nolan, and K. A. Emanuel, 2010: Thermodynamic control of tropical cyclogenesis in environments of radiative-convective equilibrium with shear. *Quart. J. Roy. Meteor. Soc.*, **136**, 1954–1971, https://doi.org/10.1002/qj.706.

Reed, K. A., and D. R. Chavas, 2015: Uniformly rotating global radiative-convective equilibrium in the Community Atmosphere Model, version 5. *J. Adv. Model. Earth Syst.*, **7**, 1938–1955, https://doi.org/10.1002/2015MS000519.

Riehl, H., 1945: Waves in the easterlies and the polar front in the tropics. University of Chicago Dept. of Meteorology Misc. Rep. 17, 79 pp.

——, 1951: Aerology of tropical storms. *Compendium of Meteorology*, T. F. Malone, Ed., Amer. Meteor. Soc., 902–913.

——, and N. M. Burgner, 1950: Further studies of the movement and formation of hurricanes and their forecasting. *Bull. Amer. Meteor. Soc.*, **31**, 244–253, https://doi.org/10.1175/1520-0477-31.7.244.

Rotunno, R., and K. A. Emanuel, 1987: An air–sea interaction theory for tropical cyclones. Part II. *J. Atmos. Sci.*, **44**, 542–561, https://doi.org/10.1175/1520-0469(1987)044<0542:AAITFT>2.0.CO;2.

Sobel, A. H., J. Nilsson, and L. M. Polvani, 2001: The weak temperature gradient approximation and balanced tropical moisture waves. *J. Atmos. Sci.*, **58**, 3650–3665, https://doi.org/10.1175/1520-0469(2001)058<3650:TWTGAA>2.0.CO;2.

Sugi, M., Y. Yamada, K. Yoshida, R. Mizuta, M. Nakano, C. Kodama, and M. Satoh, 2020: Future changes in the global frequency of tropical cyclone seeds. *SOLA*, **16**, 70–74, https://doi.org/10.2151/sola.2020-012.

Tang, B., and K. Emanuel, 2010: Midlevel ventilation's constraint on tropical cyclone intensity. *J. Atmos. Sci.*, **67**, 1817–1830, https://doi.org/10.1175/2010JAS3318.1.

——, and ——, 2012: Sensitivity of tropical cyclone intensity to ventilation in an axisymmetric model. *J. Atmos. Sci.*, **69**, 2394–2413, https://doi.org/10.1175/JAS-D-11-0232.1.

Tippett, M. K., S. Camargo, and A. H. Sobel, 2011: A Poisson regression index for tropical cyclone genesis and the role of large-scale vorticity in genesis. *J. Climate*, **24**, 2335–2357, https://doi.org/10.1175/2010JCLI3811.1.

Vecchi, G. A., and Coauthors, 2019: Tropical cyclone sensitivities to CO_2 doubling: Roles of atmospheric resolution, synoptic variability and background climate changes. *Climate Dyn.*, **53**, 5999–6033, https://doi.org/10.1007/s00382-019-04913-y.

Vu, T.-A., C. Kieu, D. Chavas, and Q. Wang, 2021: A numerical study of the global formation of tropical cyclones. *J. Adv. Model. Earth Syst.*, **13**, e2020MS002207, https://doi.org/10.1029/2020MS002207.

Wing, A. A., S. J. Camargo, and A. H. Sobel, 2016: Role of radiative-convective feedbacks in spontaneous tropical cyclogenesis in idealized numerical simulations. *J. Atmos. Sci.*, **73**, 2633–2642, https://doi.org/10.1175/JAS-D-15-0380.1.

Xu, K.-M., and K. A. Emanuel, 1989: Is the tropical atmosphere conditionally unstable? *Mon. Wea. Rev.*, **117**, 1471–1479, https://doi.org/10.1175/1520-0493(1989)117<1471:ITTACU>2.0.CO;2.

Yang, W., T.-L. Hsieh, and G. A. Vecchi, 2021: Hurricane annual cycle controlled by both seeds and genesis probability. *Proc. Natl. Acad. Sci. USA*, **118**, e2108397118, https://doi.org/10.1073/pnas.2108397118.